Palacký University, Olomouc
Faculty of Sciences
Department of Physical Chemistry

High-resolution scanning probe microscopy: tool for chemical analysis of molecules on surfaces

Habilitation Thesis

Pavel Jelínek

I declare that I carried out this habilitation thesis independently, and only with the cited sources, literature and other professional sources.

In Olomouc February 22, 2017

. . . .

P. Jelínek

Acknowledgement

First I would like to thank my wife Adriana and my parents Věra and František, for their support and patience. My kids Ella, Frida, Vesna and František Jr. for the light they bring into my life everyday. I would like to specially thank to my colleagues from the Institute of Physics of CAS for fundamental contribution to this thesis, for deep-insight discussions and critical comments: M. Švec, M. Ondráček, V. Cháb, J. Kočka, H. Vazquez, P. Hapala, O. Krejčí, O. Stetsovych, B. de la Torre, Z. Majzik, M. Moro, P. Mutombo, J. Berger, V. Zobač, M. Telychko, J. Hellerstedt, T. Chutora, J. Lopez Redondo and A. Cahlík. Special thanks to M. Ondráček for carefull review of the thesis. I would like to thank to Ivo Starý and his colleagues for providing new ideas and exciting discussions about molecular systems. I'm indebted to following colleagues for inspired discussions and critical comments J. Repp, F. Albrecht, R. Temirov, F.J. Tautz, J. van der Lit, N. J. van der Heijden, I. Swart, N. Pavliček, L. Gross, N. Moll, G. Meyer, F. Flores, J. Ortega, P. Pou, R. Peréz, M. Ternes, Y. Sugimoto, S. Morita, O. Custance, P. Liljeroth, F. Schulz, F.J. Giessibl, K.J. Franke, I.J. Pascual, A. Garcia-Lekue, T. Fredericksen and A. Arnau.

Contents

Abstract

This thesis reports on both experimental and theoretical works which provide deeper insight into the mechanism of the high-resolution imaging of molecules on surfaces under ultra high vacuum with a functionalized probe by means of AFM, STM and IETS techniques and their applications. In introduction, the current status and challenges of the high-resolution imaging are briefly summarised. The mechanisms of the high-resolution imaging using a simple mechanistic model *[Hapala 2014, Hapala 2014a, Krejčí 2017]* are discussed in the first section. The model provides not only the deep understanding of the origin of the high-resolution AFM *[Hapala 2014,Hapala 2014a ,Lit 2016]*, STM *[Hapala 2014, Krejčí 2017]* and IETS-STM *[Hapala 2014]* contrasts, but it also allows to simulate high-resolution SPM images in very efficient way. Possibility of chemical recognition of single molecules on surface [Heijden 2016] and high-resolution imaging *[Iwata 2015]* at room temperature are also discussed. The second section contains description of two novel methods, which allow to resolve charge distribution *[Albrecht 2015]* and electrostatic potential *[Hapala 2016]* within single molecules with sub molecular resolution. In the third section, combined experimental and theoretical study of self-assembling processes on different surfaces *[Berger 2016]* , on-surface chemical reactions *[Kocić 2016]* and transformation of molecular chirality *[Stetsovych 2016]* on metal surfaces induced by thermal annealing is discussed. The last Chapter describes experimental and theoretical analysis of the weak intermolecular interaction and the electron transport between two molecules placed on tip apex and surface *[Corso 2015]*. Beyond that, the thesis includes a brief discussion of perspectives and remaining challenges of the high-resolution scanning probe microscopy.

List of publications relevant to the thesis

[Hapala 2014] P. Hapala, G. Kichin, Ch. Wagner, F. S. Tautz, R. Temirov, P. Jelínek *Mechanism of high-resolution STM/AFM imaging with functionalized tips* **Phys. Rev. B** 90 (2014) 085421(1) - 085421(9).

[Hapala 2014a] P. Hapala, R. Temirov, F. S. Tautz, P. Jelínek *Origin of High-Resolution IETS-STM Images of Organic Molecules with Functionalized Tips* **Phys. Rev. Lett.** 113 (2014) 226101(1) - 226101(5).

[Albrecht 2015] F. Albrecht, J. Repp, M. Fleischmann, M. Scheer, M. Ondráček, P. Jelínek *Probing Charges on the Atomic Scale by Means of Atomic Force Microscopy* **Phys. Rev. Lett.** 115 (2015) 076101-1 - 076101-5.

[Corso 2015] M. Corso, M. Ondráček, Ch. Lotze, P. Hapala, K. J. Franke, P. Jelínek, J. I. Pascual *Charge Redistribution and Transport in Molecular Contacts* **Phys. Rev.**

Lett. 115 (2015) 136101(1) - 136101(5).

[Iwata 2015] K. Iwata, Sh. Yamazaki, P. Mutombo, P. Hapala, M. Ondráček, P. Jelínek, Y. Sugimoto *Chemical structure imaging of a single molecule by atomic force microscopy at room temperature* **Nat. Commun.** 6 (2015) 7766(1) - 7766(6).

[Berger 2016] J. Berger, K. Kosmider, O. Stetsovych, M. Vondráček, P. Hapala, E. J. Spadafora, M. Švec, P. Jelínek *Study of Ferrocene Dicarboxylic Acid on Substrates of Varying Chemical Activity* **J. Phys. Chem. C** 120 (2016) 21955 - 21961.

[Heijden 2016] N. J. van der Heijden, P. Hapala, J. A. Rombouts, J. van der Lit, D. Smith, P. Mutombo, M. Švec, P. Jelínek, I. Swart *Characteristic Contrast in* Δf_{min} *Maps of Organic Molecules Using Atomic Force Microscopy* **ACS Nano** 10 (2016) 8517 - 8525.

[Lit 2016] J. van der Lit, F. Di Cicco, P. Hapala, P. Jelínek, I. Swart *Submolecular Resolution Imaging of Molecules by Atomic Force Microscopy: The Influence of the Electrostatic Force* **Phys. Rev. Lett.** 116 (2016) 096102-1 - 096102-5.

[Hapala 2016] P. Hapala, M. Švec, O. Stetsovych, N. J. van der Heijden, M. Ondráček ,J. van der Lit, P. Mutombo, I. Swart, P. Jelínek *Mapping the electrostatic force field of single molecules from high-resolution scanning probe images* **Nat. Commun.** 7 (2016) 11560(1) - 11560(8).

[Kocić 2016] N. Kocić, X. Liu, S. Chen, S. Decurtins, O. Krejčí, P. Jelínek, J. Repp, S.-X. Liu *Control of Reactivity and Regioselectivity for On-Surface Dehydrogenative Aryl-Aryl Bond Formation* **J. Am. Chem. Soc.** 138 (2016) 5585 - 5593.

[Stetsovych 2016] O. Stetsovych, M. Švec, J. Vacek, J. Vacek Chocholoušová, A. Jančařík, J. Rybáček, K. Kosmider, I. G. Stará, P. Jelínek, I. Starý *From helical to planar chirality by on-surface chemistry* **Nat. Chem.** 9, (2017) 213-218.

[Krejčí 2017] O. Krejčí, P. Hapala, M. Ondráček, P. Jelínek *Principles and simulations of high-resolution STM imaging with a flexible tip apex* **Phys. Rev. B** 95 (2017) 045407(1) - 045407(9).

Chapter 1

Introduction

The analysis, control and modification of molecules, surfaces and nanostructures are among the great challenges of the last few years. Nanoprobe techniques such as Scanning Tunneling Microscopy (STM) [1] and Atomic Force Microscopy (AFM) [2] provide not only a variety of experimental information at the atomic scale, they are also widely used as an assembly tool for creating potential nanotechnology devices using both contact and non-contact modes of the operation [3, 4].

The invention of STM and AFM more than 30 years ago were two significant milestones initiating the era of Nanoscience and Nanotechnology. The possibility to image and manipulate individual atoms or molecules on surfaces opened new perspectives for control and understanding of the physical and chemical processes at the atomic scale. These Scanning Probe Microscopy (SPM) techniques have found wide applications in Nanotechnology and other research areas such as Surface Physics and Chemistry, Tribology, Molecular and Cell Biology etc. It is evident that the further development of these Scanning Probe tools will have a large impact on many scientific areas.

Recently, several new experimental techniques with atomic resolution derived from standard AFM or STM techniques, such as inelastic electron tunneling spectroscopy (IETS) [5], Kelvin Probe Force Microscopy [6] and combined STM/AFM measurements [7], have been introduced. One of the most remarkable and exciting achievements in the SPM field in the last years is the unprecedented sub-molecular resolution of both atomic and electronic structures of single molecules deposited on solid state surfaces. Despite its youth, the technique has already brought many new possibilities to perform different kinds of measurements, which cannot be accomplished by other techniques. This opens new perspectives in advanced characterization of physical and chemical processes and properties of molecular structures on surfaces. Nevertheless the complexity of this technique requires new theoretical approaches, where a relaxation of the functionalized probe is considered.

While atomic resolution on different kinds of surfaces became routinely achieved, reaching at least a moderate spatial resolution on single molecules was very difficult. Usually molecules were only imaged as featureless objects lacking any signature of internal structure. Indeed the internal resolution of molecules on surfaces by means of SPM remained a great challenge for many years.

The situation has changed drastically with the discovery of enhanced molecular contrast using a proper tip functionalization a few years ago. The unprecedented sub-molecular resolution of organic molecules on solid state surfaces achieved under ultra high vacuum (UHV) by both STM and AFM modes represents one of the most remarkable and exciting achievements in the SPM field in the last years. The possibility to achieve detailed information about the chemical structure of a single molecule, a priori unknown, on surfaces opens completely new possibilities in Surface Science, Chemistry, Biology and Nanoscience.

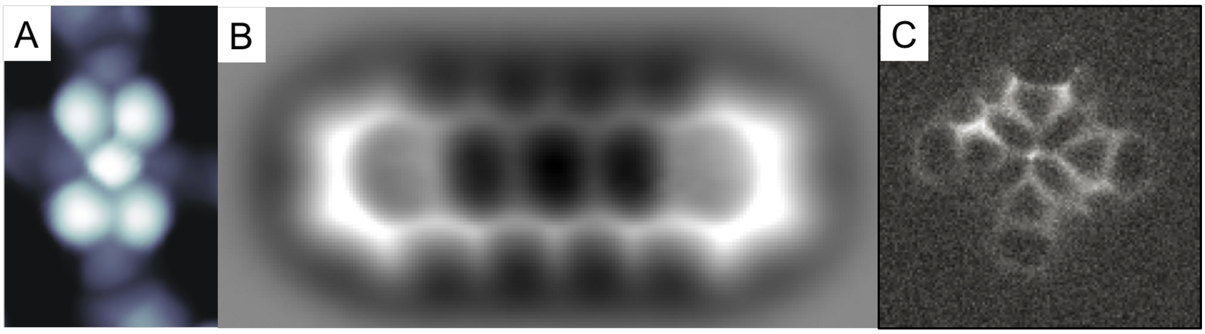

Figure 1.1: **Examples of high resolution STM, AFM and IETS-STM images of molecules obtained with functionalized tips:** (a) Experimental constant height HR-STM dI/dV figure of PTCDA/Au(111) obtained with CO-tip at V_{bias} = -1.6 V with respect to the sample (adopted from [8]). (b) Constant height nc AFM simulations of a pentacene molecule on a NaCl thin film acquired with CO-tip (adopted from [9]). (c) constant-height IETS-STM image of CoPc molecule on Ag(110) surface with CO-tip (adopted from [10])

The main obstacle to achieving sub-molecular contrast is a relatively weak signal-to-noise ratio detected during measurements. An important ingredient for achieving high-resolution imaging is proper decoration of the tip apex by an atom or molecule intentionally/accidentally picked up from the surface, which serves to significantly amplify the detected signal.

I believe that the basic principles of the mechanism providing the high-resolution AFM/STM contrast (i.e. lateral relaxation of a frontier atom/molecule on tip apex) can be also applied to the understanding of atomic contrast observed on metal surfaces using electrochemical STM [11], and STM operating in the contact mode [12, 13, 14], or the recently observed atomic contrast of non-contact AFM in liquids [15, 16].

Probably the first evidence of the contrast enhancement due tip functionalization was reported by Jascha Repp and his colleagues in 2005 [17]. In this seminal paper, they presented real space STM imaging of molecular orbitals of a pentacene molecule deposited on an insulator layer. They demonstrated that the contrast was significantly increased by the presence of a pentacene molecule located on the tip apex. This effect was later explained theoretically [18] as a consequence of the selection rules governing the tunnelling process across the STM junction.

In 2008, Ruslan Temirov and his colleagues [8] discovered that an admission of hydrogen molecules into the UHV chamber induces the significant enhancement of molecular contrast observed in STM images when tip is brought very close to an inspected surface. The STM images contain characteristic sharp edges, which mimics very well the molecular structure of perylenetetracarboxylic dianhydride (PTCDA) molecules, see Fig. 1.1 (a). They attributed this effect to the presence of the hydrogen molecules in the tunnelling junction preferentially bounded to a metallic tip apex. Afterwards, they demonstrated that a variety of other functionalized tips intentionally decorated by atoms (Xe) or molecules (CH_4, CO) enable resolution of chemical structures of large organic molecules deposited on metallic surfaces with unprecedented details [19, 20]. For

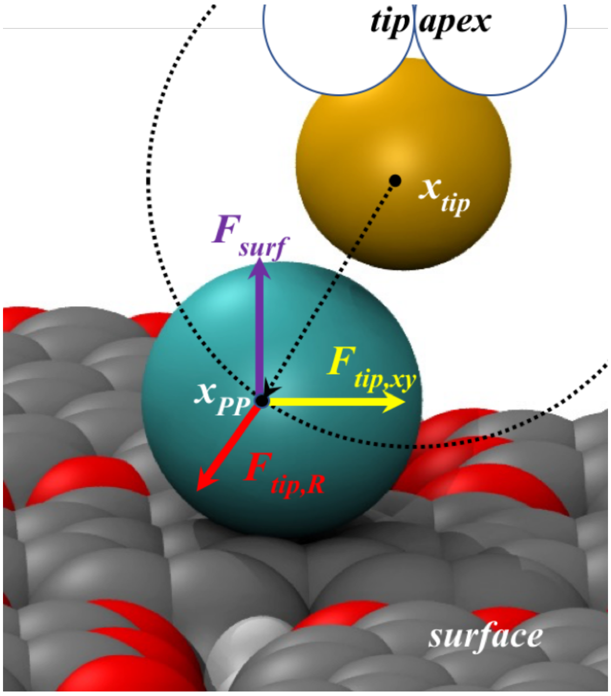

Figure 1.2: **Schematic representation of forces acting on the probe particle representing the functionalized tip in the mechanistic PP-model:** The probe particle (green ball) experiences different interactions from the surface F_{Surf}, the tip apex $F_{Tip,R}$ and lateral force $F_{Tip,xy}$; adopted from [32].

historical reasons, this technique is known as scanning tunneling hydrogen microscopy (STHM).

One year later, Leo Gross and his colleagues [9] published their seminal work presenting high-resolution AFM images of pentacene molecule, see Fig. 1.1 (b), deposited on an insulating thin film, employing so called non-contact (nc) AFM mode [3, 4]. The key step was a controlled functionalization of metallic tip apex with a single carbon monoxide (CO) molecule [21]. The high-resolution AFM images contain sharp edges revealing clearly the internal chemical structure of the molecule similarly to the STHM technique. This discovery has stimulated research activities of many groups, particularly in the community of nc-AFM [22], to achieve, understand and further explore this high-resolution imaging. This effort has brought significant advances not only in the characterisation of molecular structures on surfaces [23, 24, 25] but also in the understanding of chemical transformation on surfaces [26, 24, 27] or investigating weak van der Waals interactions [28, 29, 30].

Finally in 2014, Wilson Ho's group presented an alternative approach to achieve high-resolution contrast by employing IETS channel [10]. They mapped out variations of the IETS signal of the frustrated translational mode of CO molecule placed on the tip apex while scanning over molecules deposited on a metal surface. In close tip-sample distances, the IETS maps reveal sharp contrast mimicking the molecular structure, in very similar manner to those observed with AFM and STM, as shown in Fig. 1.1 (c). The similarity of the contrast between different high-resolution modes indicates a common mechanism, which is responsible for the submolecular contrast [31].

Nowadays the basic mechanism of the high-resolution AFM images is fairly well understood. In their landmark paper [9], Gross and his colleagues attributed the origin of high-resolution AFM imaging to Pauli repulsion [33], which dominates the tip-sample interaction at close distances. Later Gross and Moll also pointed out the importance of a lateral bending of the functionalized tip apex [34]. This effect was further elaborated by others [35, 36, 37, 32, 38]. About same time in 2014, two groups independently proposed similar mechanistic models [32, 38], which can explain the main ingredients of the AFM imaging mechanism. In the approach devised by Hapala et. al [32], we introduced the concept of a so-called probe particle (PP) model, where a flexible molecule/atom located at the tip apex is represented by a single particle, as schematically depicted in Figure 1.2. The position of the probe particle is optimised according to classical force field combining van der Waals, electrostatic and Pauli forces acting between tip and sample. This model provides not only a detailed understanding of the imaging mechanisms with functionalized tips but also represents a very efficient simulation tool (available online [39]). These days, there are several more sophisticated theoretical approaches available for the high-resolution AFM modelling extending basics ideas of the PP model and employing inputs from total energy density functional theory (DFT) calculations [31, 40, 41, 42].

On the other hand, the precise origin of the STHM and IETS-STM imaging mechanism remained long under debate [19, 43]. Nevertheless we showed that the mechanistic PP-model for high-resolution AFM images [32] can be extended to both STM [32, 44] and the IETS-STM mode [31].

Chapter 2

Results and Discussions

2.1 High-resolution AFM imaging

Figure 2.1 shows an evolution of simultaneously acquired AFM and STM images of PTCDA molecules on Ag(111) surface during the approach of a tip decorated with a single Xe atom [45, 46]. In the far tip-sample distance regime, the AFM contrast consists of a featureless oval rendering molecular contour. In intermediate tip-sample distances, the AFM contrast changes significantly clearly revealing characteristic benzene rings of PTCDA molecules. In very close distances, one can observe a characteristic bond sharpening, which is later accompanied with a contrast inversion. In particular, areas corresponding to the central part of benzene rings become more repulsive compared to those corresponding to molecular bonds and atoms. The contrast inversion effect is better visible in 3D plots of AFM images, shown in the left column of Figure 2.1.

The characteristic evolution of the AFM contrast is driven by an interplay between different force components acting between functionalized tip and sample: attractive van der Waals (vdW), electrostatic and repulsive Pauli forces. What can be skipped is the chemical force reflecting a formation of covalent/metal bond between outermost atoms of tip apex and sample. The presence of an inner molecule/atom at the tip apex reduces significantly chemical reactivity with respect to bare metallic tips. Thus we can exclude a formation of strong chemical bond between tip and sample [47, 48]. In principle, this substantially simplifies the theoretical description of tip-sample interaction avoiding demanding quantum mechanical calculations to capture the formation of chemical bonds.

Based on these assumptions, we introduced the mechanistic probe particle model [32], which capture the main ingredients of the AFM imaging mechanism. In this model, the probe particle representing a an atom/molecule loosely attached to the tip apex, as schematically depicted in Figure 1.2. The position of the probe particle is optimised according to classical force field combining van der Waals, electrostatic and Pauli forces acting between tip and sample during the tip approach. The PP-AFM can reproduce very well evolution of AFM contrast for range of tip-sample distances, as can be seen from comparison of Figures 2.1 and 2.2.

The absence of chemical bonding plays a fundamental role in the origin of the high-resolution imaging. It enables stable operation of the probe in the repulsive regime without undergoing irreversible changes. Thus the chemical inertness of the probe is an important prerequisite to achieve high-resolution contrast. Noteworthily, the functionalized molecule/atom attached to the metallic tip base is mechanically the softest

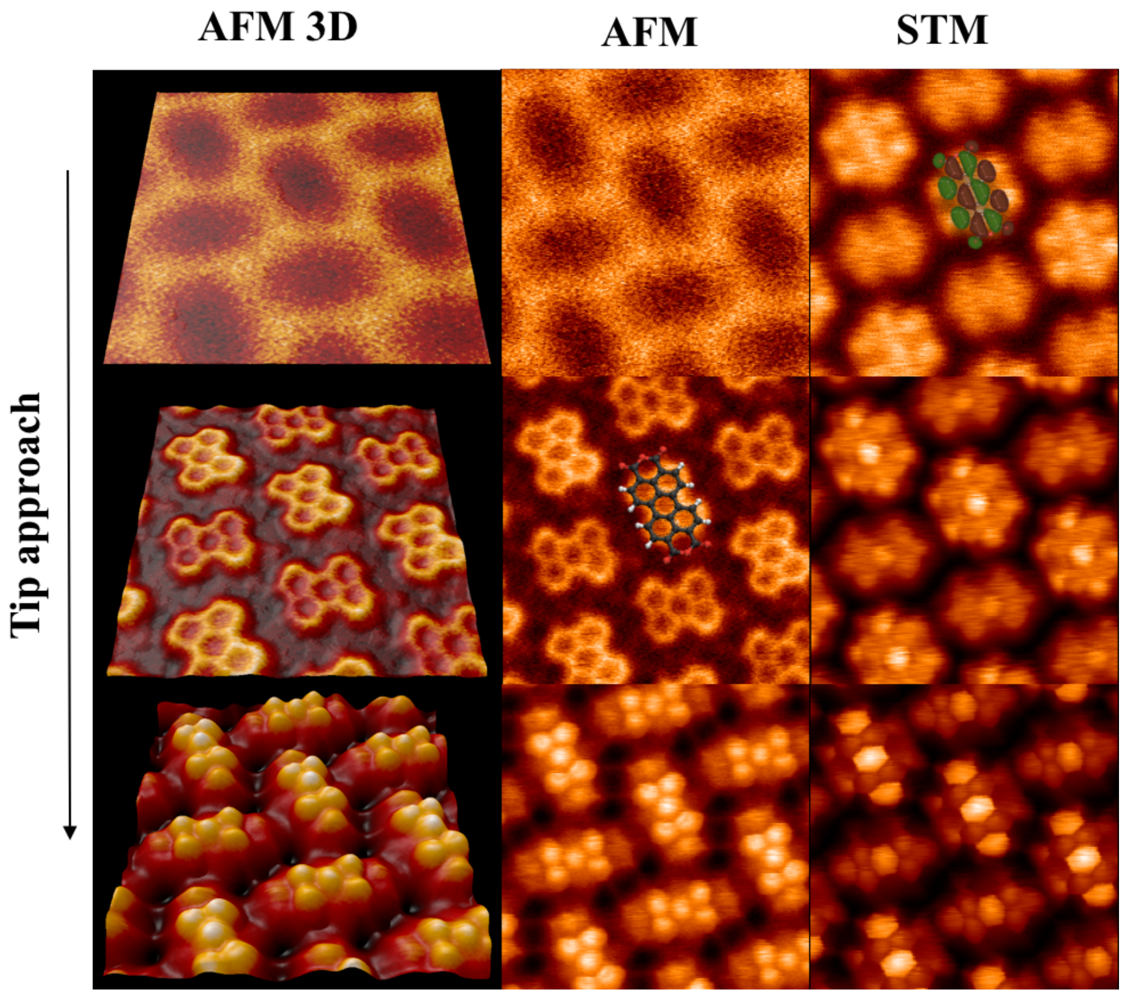

Figure 2.1: **Evolution of high resolution AFM/STM contrast of PTCDA molecules on Ag(111) surface during approach of Xe-terminated tip:** (Left column) series of constant height AFM images rendered in 3D for different tip sample distances. (Middle column) the same AFM images as these shown in the left column, but plotted in 2D perspective. Atomic structure of PTCDA molecule is superimposed over the AFM image. (Right column) series of constant height STM images acquired simultaneously with AFM channel [45]. Calculated LUMO orbital of PTCDA molecule is also displayed to show that it coincides well with the STM contrast observed in far distances.

part of the whole tip-sample system. Consequently the mechanical stress induced by proximity of tip to surface is released mostly via a lateral relaxation of the probe particle and additional relaxation of the surface can typically be neglected. Of course, this assumption does not hold for complex non-planar molecules, which makes their high-resolution imaging and its interpretation more difficult.

Let us discuss the role of each force component along the tip approach axis. In far tip-sample distances, vdW forces prevail giving rise to the blunt contrast over a molecule. On the other hand, in close tip-sample distances, it is the Pauli repulsion, which gives rise to the appearance of sharp edges in images. The sharp edges correspond to extremes (saddle points) of the potential energy surface, which the probe particle experiences in a given tip-sample distance [32, 38]. The saddle points are typically formed over atoms or bonds where the Pauli repulsion fully compensates the attractive

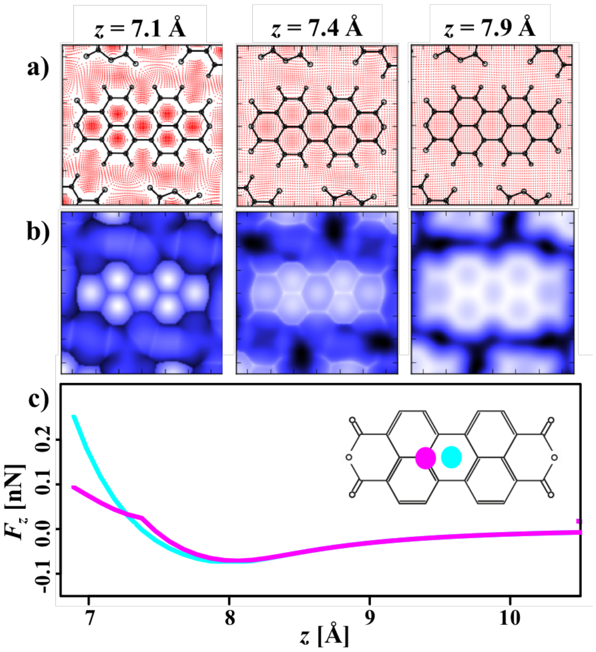

Figure 2.2: **Calculated high-resolution AFM images of herringbone monolayer of PTCDA molecules deposited on Au(111) surface at different distances with the mechanistic PP-model:** a) lateral relaxation of the probe particle; b) AFM (frequency shift) images and; c) calculated vertical force F_z as a function of the tip-sample distance z measured over a carbon atom (pink) and the center of a benzene ring (turquoise; shown on inset of Figure c); adopted from [45].

forces at a given tip-sample distance. At this distance, probe particle trajectories start to branch (bifurcate) to one or the other side of the saddle, as schematically depicted on Figure 2.3 (b). While Pauli repulsion defines the distance where the bifurcation appears and the manifold, on which the probe particle slides upon further approach, the actual strength of Pauli repulsion is not very important for an apparent lateral position of the sharp features in the image (for detailed discussion of this effect see supplement of [46]). It is the electrostatic force, which can be both attractive and repulsive at different parts over an inspected molecule, responsible for variation of the lateral position of the intramolecular sharp edges [31, 46] as it will be discussed later.

In summary, we can say that the sharp features appearing in the AFM images always coincide with the borders of neighbouring basins in the potential energy surface. In other words, they correspond to the narrow areas, where the magnitude and direction of the lateral relaxation of the probe particle changes strongly upon small variations of the position of the tip relative to the sample (see Figure 2.3). Since the lateral and vertical relaxations of the probe particle are closely coupled, in the area between the neighbouring basins, the vertical position of the probe particle also becomes very sensitive to the precise position of the tip. Consequently, it causes the sharp image features in the AFM images, see Figure 2.3 (b).

2.1.1 Do the sharp lines always represent true bonds?

The position of sharp lines in the high-resolution AFM images typically coincides with intramolecular bonds between atoms of a given molecule. Hence the appearance of the sharp lines tempts one to automatically interpret them as the true bonds. However,

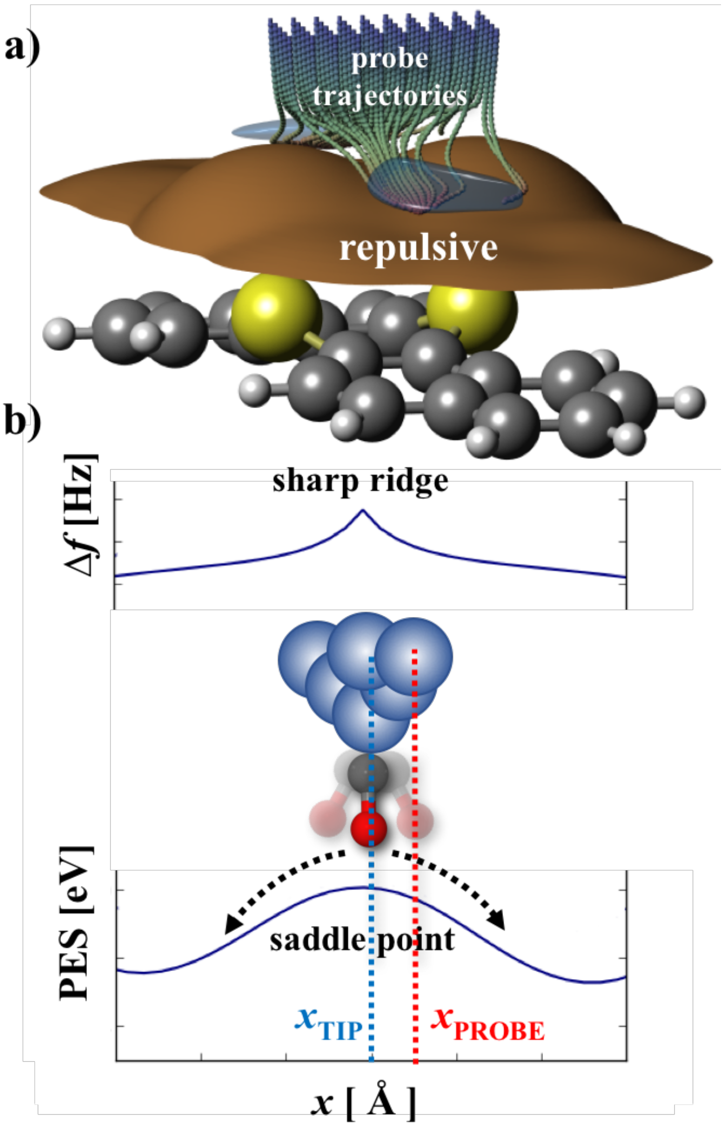

Figure 2.3: **Explanation of the sharpening of AFM contrast as consequence of lateral relaxation of probe particle in close distances:** (a) Schematic view of the probe particle trajectory during tip approach represented by individual threads, dominated by the Pauli repulsion energy. (b) Appearance of the sharp edge in the frequency shift Δf signal due to convex shape of the potential surface energy (PES) landscape causing the probe particle relaxation at close distances; adopted from [32].

N. Pavliček et al. [49] found a pathological case, where the sharp edges can be also seen between two sulphur atoms, where there is no chemical bond established. This experimental evidence we can also reproduce by our PP-model [32], see Figure 3 in [32]. On the other hand, Zhang et al. [50] published high-quality AFM images of weakly bonded assemblies of guanine molecules on a metal surface, revealing clear sharp edges observed between the molecules. In addition, total energy density functional theory (DFT) calculations revealed enhanced accumulation of the electron density in locations, where the sharp lines were experimentally observed. Based on this argument, they correlated these sharp lines to intermolecular hydrogen bonds formed between guanine molecules. Sweetman et al. observed intermolecular sharp lines in high-resolution AFM images between naphthalene tetracarboxylic diimide molecules [51], matching expected positions of intermolecular hydrogen bonds. The fact that both experimental AFM contrasts [50, 51] can be reproduced well by our mechanistic PP-model [32] without taking explicitly into account distribution of the electron density opened a lively debate about the origin and the correct interpretation of these sharp intramolecular features.

To tackle this problem, Hamalainen et al. [38] investigated a molecular system, where intermolecular bonds should or should not be present between neighbouring molecules. They found that sharp intermolecular features are detected in both regions. This finding clearly demonstrates that the intermolecular contrast cannot be automatically interpreted as true intermolecular bonds. These finding were also supported by theoretical modelling [38, 52]. Furthemore, very similar conclusions were also found in others works [53, 54].

Thus the possibility to conclusively identify the true intramolecular hydrogen bonds remains an open challenge. To clearly discriminate true bonds, one can think about simultaneous application of different techniques in a multi-pass mode. For example, one can employ first the high-resolution AFM/STM imaging to detect the position of sharp lines. Next, one can try to detect the presence of the IETS signal [5] characteristic for weak intermolecular hydrogen bonds in the marked intermolecular area. It has been shown recently that the IETS signal can be enhanced by a proper tip apex functionalization [55], which can make the scheme feasible.

2.1.2 Impact of the electrostatic force on the AFM contrast

We already mentioned that the high-resolution AFM imaging mechanism is driven by the interplay between attractive van der Waals (vdW), electrostatic and repulsive Pauli forces acting between the functionalized tip and sample. Originally, only vdW and Pauli forces were considered in theoretical explanations [9, 33, 38, 32]. Therefore there is a question namely, what is the role of the electrostatic force in the imaging mechanism? The strength of the electrostatic force depends on the charge density distribution (polarity) on probe and surface. Indeed, for non polar organic molecules, fairly good agreement between experimental and simulated AFM images can be achieved without the inclusion of the electrostatic force [32], see also Figure 2.2. However, detailed analysis of different cases revealed that agreement with experimental evidences can be substantially improved, when the electrostatic force is included in the PP-model [31, 45].

What is more, the AFM contrast of polar molecules with strong internal charge redistribution can significantly change [56], even when scanning with different functionalized tips [46, 57], as shown on Figure 2.4. We demonstrated that the effect is caused by a displacement of the probe particle by the electrostatic field of the probed molecules during scanning. In other words, the movement of the probe particle induces the distortions of the positions of atoms and bonds seen in the high-resolution images, as shown on Figure 2.5. This effect allows for mapping of the electrostatic field in the vicinity of the investigated molecules [46]. As another example, we investigated AFM images of an ordered monolayer of bis-(para-benzoic acid) acetylene molecules acquired with different tip terminations: Xe and CO [57]. We found that the brightness and contours of the AFM contrast are significantly affected by the tip termination. Using the PP-model including the electrostatic interaction, we could deduce that the charge of the tip and its electrostatic interaction with the sample is crucial in determining the contrast and the tip relaxations. The impact of the electrostatic force on the AFM

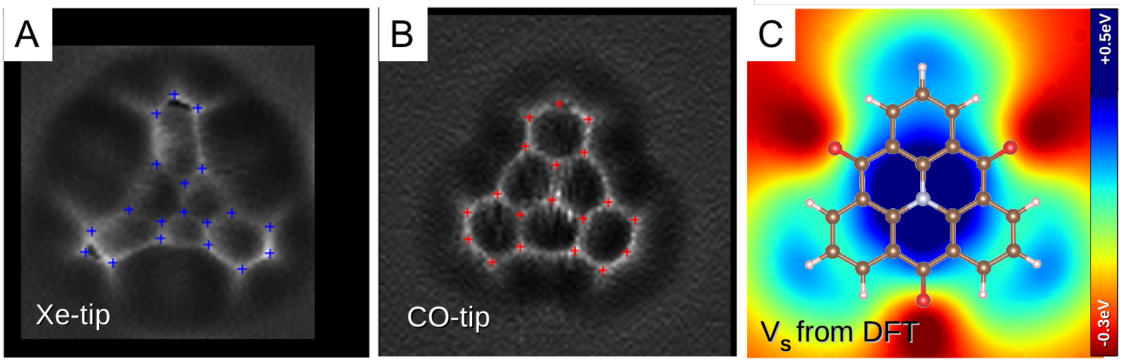

Figure 2.4: **Variation of the high-resolution AFM contrast of TOAT molecule acquired with different probes.** (a) Constant height high-resolution AFM image acquired with Xe-tip; (b) Constant height high-resolution AFM image acquired with CO-tip; (c) Calculated Hartree potential above TOAT molecule obtained from DFT simulations; adopted from [46].

contrast was also discussed in detail by Guo et al. [41] for π-conjugated molecules and Ellner et al. [40] for ionic surfaces.

In the PP-model, the electrostatic force is calculated from the Hartree surface potential obtained from fully relaxed total energy DFT calculations of a molecule on surface and an effective charge density on the probe particle [31], see also scheme depicted on Figure 2.6. The effective PP charge density can be approximated by different multipoles [46, 40] including monopole, dipole or quadrupole. What is more, the charge density distribution can be significantly affected by charge transfer between atom/molecule on the apex and the metallic tip base. Thus it is important to understand and to correctly determine the charge distribution of functionalized tips. Comparisons between various experimental evidences and modelling revealed [46, 57, 58] that a CO-terminated tip has only a very weak, mostly negative, charge, while a Xe-terminated tip is positively polarised.

Ellner et al. [40] showed that overall picture can be more complex. They found that the electrostatic field of the CO-terminated metallic tip can be described as a superposition of two fields originating from the metal base tip and the CO molecule. The interplay of these two fields with opposite sign is fundamental to capture the contrast evolution of a Cl vacancy in bilayer NaCl on Cu(111) along the tip approach axis. While a dipole with its positive pole at the metallic tip dominates at far distance, an opposite field located on the CO molecule prevails in close distances. Very recently, we have performed an analysis of a chiral AFM contrast obtained at far distance over a strongly polar water tetramer deposited on NaCl thin film with a CO-terminated tip. We demonstrated that the contrast can be well explained by a slightly negative quadrupole (i.e. with the negative lobe pointing towards the surface) charge model for the probe particle [59]. It is evident that the charge distribution on different functionalized tips is still not completely understood and calls for more experimental and theoretical investigations.

It is also desirable to define new atomic or molecular candidates for tip functionalization [60, 61]. The main factors causing the wide usage of CO or Xe functionalized tips are i) a well-defined and reproducible recipe for their preparation [62, 63, 64, 21], ii) flexibility and stability of the molecule/atom on a metallic tip apex. However, the charge of such tips cannot be controlled easily. Better sensitivity could be achieved

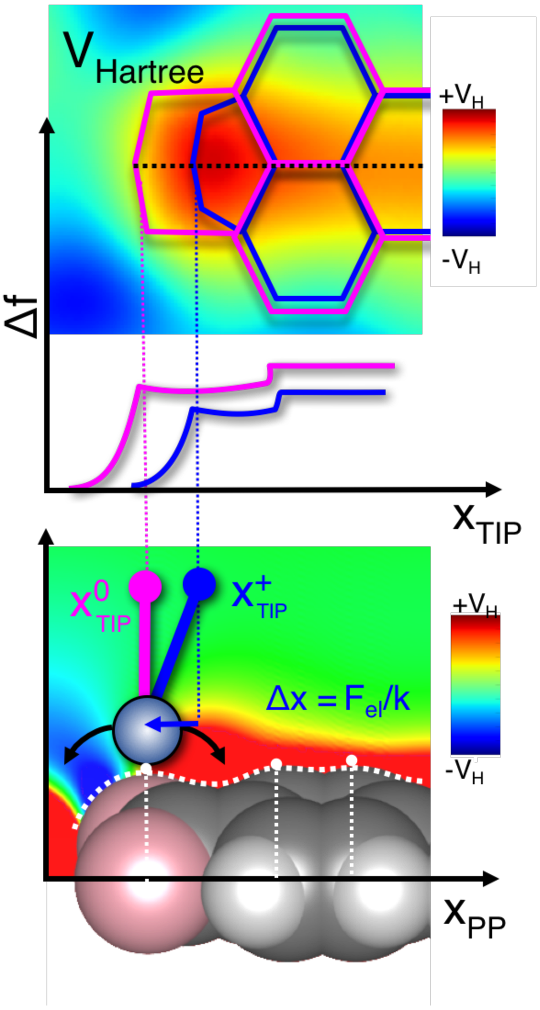

Figure 2.5: **Schematic picture demonstrating the effect of lateral bending of the probe particle on the position of the sharp edges in high-resolution.** (Upper) Blue and pink lines represent different positions of the sharp edges observed in high-resolution images acquired with the probe particles experiencing different lateral (electrostatic) force. The position of the sharp edges in Δ f signal (AFM channel) changes accordingly. (Lower) Sideview of the lateral position of the probe particle x_{PP} with respect to the tip apex x_{TIP} experiencing a different lateral force at a saddle point. Background image renders calculated Hartree potential of a scanned (PTCDA) molecule, which induces the lateral bending Δx of the charged probe particle [46].

with functionalized tips having either large inherent charge or better polarizability. Ideal candidates would be small molecules or functional groups which could be easily charged by applied voltage. Therefore, we need to select new tip functionalization groups with tuneable charge/dipole/quadrupoles, easy polarisability and/or small redox potentials. Possible candidates are: hydroxyl groups, nitrile, isonitrile, nitrogen oxides, azide, quinones or transition metal chelates. Recent studies of ferrocene molecules have postulated them as an interesting candidate [65]. We also need to better understand response of functionalized tips to changing bias voltage, evaluation of their polarizability and possible charging. At the same time, we should search for the reliable and reproducible procedures for proper placement of the functional groups on the tip apex.

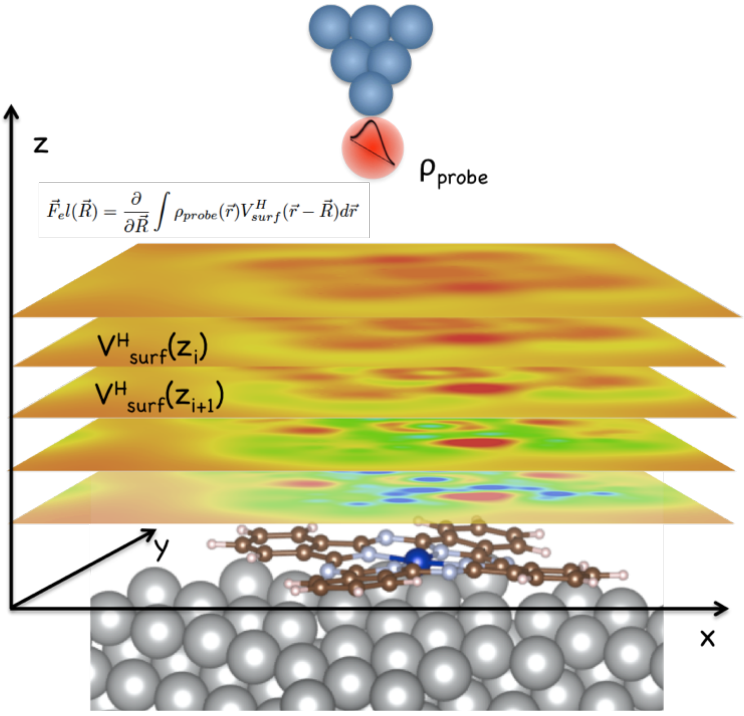

Figure 2.6: **Schematic view of the electrostatic interaction acting between an effective charge on probe and Hartree potential on surface:** The electrostatic interaction is calculated as derivative of convolution of the Hartree potential spanned on a rectangular grid obtained form total energy DFT calculations and an effective charge of the probe particle (red ball), for more details see [31].

2.1.3 Going beyond low temperature limit

The sub-molecular resolution of individual molecules brought entirely new possibilities in the study of physical and chemical properties of individual molecules or their assemblies on surfaces. So far, it has been possible to carry out these measurements only at very low temperatures close to absolute zero with specially modified probes. As we discussed above, the modification consists of controlled positioning of just a single molecule (e.g. carbon monoxide) or a noble gas atom on the apex of the metal tip. However, such tips are typically stable only at very low temperatures near to absolute zero. This condition has dramatically limited the applications of this method in terms relevant to important chemical and biological processes. For example, the possibility of imaging individual molecules on surfaces at ambient temperature represents an essential prerequisite for the study of catalytic reactions on solid surfaces at elevated temperatures.

Recently, the situation has changed in this direction. Several groups succeeded to obtain the submolecular resolution at liquid nitrogen temperature [54, 66]. Moreover, we achieved in collaboration with our colleagues from Tokyo university sub-molecular resolution even at room temperature [67]. Optimised scanning parameters enabled us a significant enhancement of the frequency shift signal. According to supporting total energy DFT calculations compared with experimental force spectroscopies, a hydroxyl terminated silicon tip was proposed to be responsible for the enhancement of the contrast. The possibility of imaging individual molecules on surfaces at ambient temperature represents essential prerequisite for the study of catalytic reactions on solid surfaces.

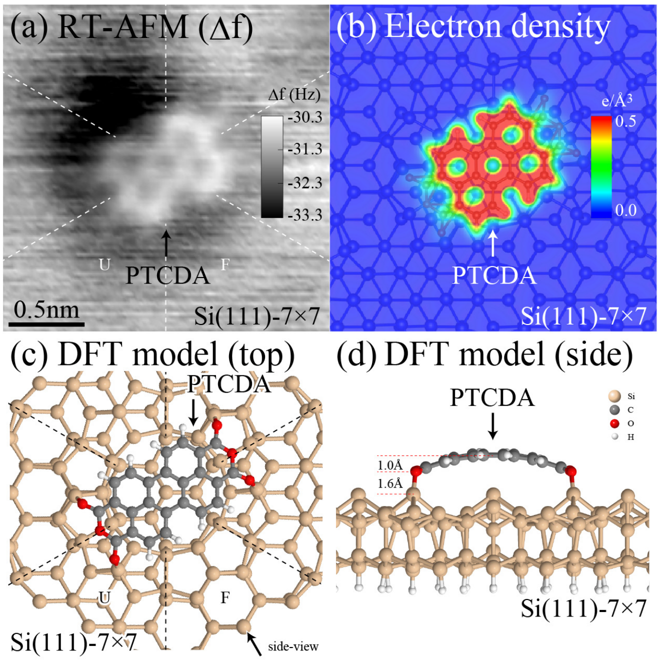

Figure 2.7: **Sub molecular resolution of PTCDA molecule on the Si(111)-7x7 surface achieved at room temperature.** a) Experimental image with the sub-molecular resolution of PTCDA molecule on the silicon surface using an atomic force microscope at room temperature, b) calculated electron density distribution above a PTCDA molecule, which contributes to the formation of high-resolution AFM images, and c, d) optimized atomic structure of PTCDA molecule after deposition on the silicon surface obtained by quantum mechanical computer simulations [67].

2.2 High-resolution STM imaging

We already discussed that a decoration of a metallic STM tip with the flexible atom or molecule leads to drastic changes of the observed STM contrast [8, 19, 68, 20]. For example, STM images of PTCDA molecules deposited on Ag(111) surface acquired in close tip-sample distances, shown on Figure 2.1 (right column), are significantly modified with respect to those in far tip-sample distances. What is more, when comparing the character of the LUMO orbital (shown on inset of Figure 2.1) with the STM contrast obtained in close distances, we can see that the STM picture has no resemblance to the typical LDOS images. Instead, it is more related to the chemical structure of PTCDA molecules. This trend holds for different functionalized tips [60].

In principle, the high-resolution STM imaging represents an experimentally less demanding way to achieve submolecular contrast than AFM or IETS-STM techniques. The STM mode posses several advantages with respect to the dynamical AFM mode [69]: (i) the tunnelling current generally behaves monotonically along the tip-sample distance; (ii) it has better signal to noise ration than the AFM mode; (iii) instrumental STM setup is less complicated than with AFM; and (iv) STM operation is much simpler than dynamical AFM mode or IETS-STM. Furthermore, it provides information about both the electronic and atomic structure of the inspected molecules. Thus, information provided by STM is, in principle, superior to AFM method. On the other hand, while the origin of the high-resolution AFM was fairly well understood soon, the high-resolution STM mechanism remained longer under debate [19, 43]. I believe that it was mainly the lack of detailed understanding of the high-resolution STM imaging mechanism, which has impeded its wider application.

The STM contrast obtained with generic metallic tips is well understood in terms of the Bardeen approach [70] and its modification derived by Chen [71, 72, 73] or even the simpler Tersoff and Hamann approximation [74]. Different simulation schemes were devised based on non-perturbative [75, 76, 77] and perturbative approaches [78, 79]. The perturbative approach is only valid in far tip-sample distances, when the contact between tip and sample is not well developed [80]. Nevertheless, all these methods assume a rigid probe without taking into account any structural tip relaxation due to tip-sample interaction. However the relaxation of the functionalized tip is crucial for the understanding of the high-resolution contrast, as we already discussed above.

Already in the original version introducing the PP-AFM model [32], we proposed a simple STM model. It describes the conductance through the STM junction via two terms: (i) the tunnelling from a metallic tip base to the probe particle T_T; and (ii) subsequent tunneling from the probe particle to the sample T_i. The tunnelling rates were described via exponential hoppings, the values of which change according to the relaxation of the PP during tip approach as discussed in [32]. Surprisingly, this very simple STM model can reasonably reproduce sharp edges frequently observed in STM images, as it was demonstrated in the case of PTCDA/Ag(111) [32]. This indicates that the relaxation of the flexible PP attached to metallic tip is most likely responsible for the peculiar submolecular STM contrast.

However, the simple STM model [32] contains one severe simplification, which prevents general application of the model to an arbitrary molecular system. It neglects completely the electronic structure in the description of the tunneling process between tip and sample. Indeed, numerous experimental evidence [8, 19, 20, 68] indicates that the STM contrast depends on experimental conditions - such as applied bias voltage or the atomic and electronic structure of STM probe and substrate. Thus, it is not surprising that inclusion of the electronic structure of both tip and sample is mandatory to understand in detail the high-resolution STM imaging with functionalized tips.

Very recently, we developed a more sophisticated but still computationally efficient STM model [44], which combines the mechanistic PP-AFM [32] and Chen's model for the tunneling process across a STM junction. The PP-AFM model introduces the PP relaxation, while the Chen's model deals with the electronic wave functions of tip and sample. The validity of the new STM model is supported by very good agreement with selected experimental STM images discussed in the original paper [44]. We showed that the new PP-STM model is able to explain experimentally observed features, which could not be properly reproduced with either the original simple model [32] or traditional STM methods. The model demonstrates that the high-resolution STM mechanism consists of the standard STM imaging [71], involving electronic states of the sample and the tip apex orbital structure, with the contrast heavily distorted by relaxation of the flexible functionalized tip apex.

To understand in detail the influence of the mechanical PP relaxation and the electronic structure on the resulting STM contrast one should analyze each of them separately. Figure 2.8(a) represents calculated STM images of a PTCDA molecule on Au(111) surface with a fixed CO-tip model. The STM contrast reveals a characteristic pattern, which transforms the original shape of the HOMO orbital into 5 stripes at each side of the molecule and 4 squares in the middle of it. This effect is the result of cancellation of the tunnelling current due to interference effects for a particular tip orbital symmetry [18]. The simulated STM contrast is very different from experimental

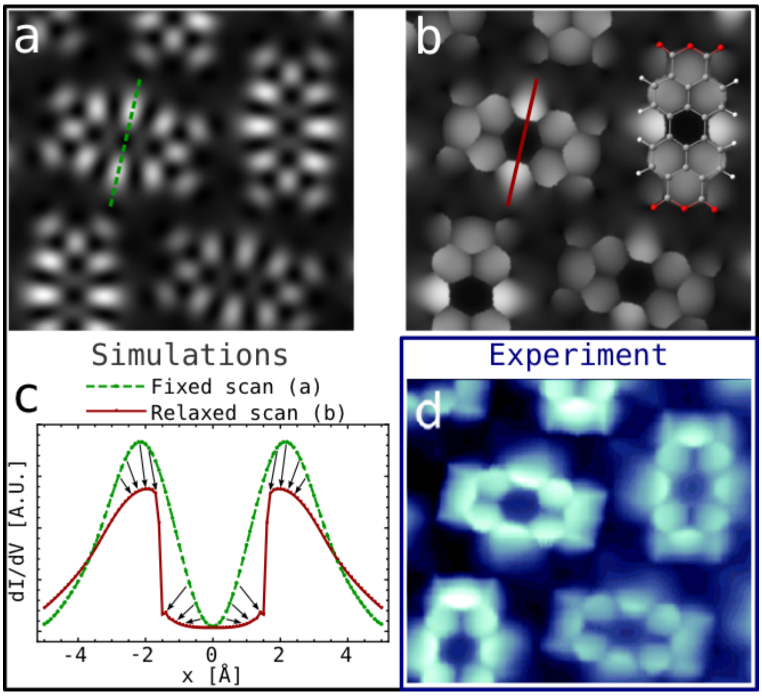

Figure 2.8: **Effect of the lateral bending of the probe particle on the STM contrast and its comparison to experimental evidence:** Calculated constant height dI/dV simulations of PTCDA/Au(111) at the energy of HOMO of PTCDA obtained with PP-STM code using p_x and p_y orbitals on the probe particle with the fixed (b) and relaxed (c) probe particle, respectively. (c) Profile lines taken above centers of PTCDA molecules as indicated in (b) and (c) by green dashed for fixed and red full line for relaxed probe particle, respectively. The arrows indicate the changes in the dI/dV signal given by the PP relaxations. (d) Experimental constant height HR-STM dI/dV figure of PTCDA/Au(111) obtained with CO tip at V_{bias} = -1.6 V [81]. For details see Krejčí et al. [44].

evidence, which is shown on Figure 2.8(d). The situation changes when we include the lateral relaxation of PP. Figure 2.8(b) represents fully optimised STM calculation, where the PP relaxation is included. The calculated STM image matches very well the experimental evidence. The impact of the PP relaxation can be better understood from the STM profile shown on Figure 2.8(c). The lateral relaxation, which the PP undergoes above a central hexagon, locates the PP in the centre of the benzene ring. This has two fundamental consequences: (i) formation of the sharp edge, where the saddle point in the potential energy surface is located; and (ii) the position of the PP remains almost unaltered while scanning over the central hexagon; consequently the STM signal remains almost constant. This gives rise to characteristic plateaus observed in the STM images.

From comparison between experimental and theoretical STM simulations, we can also learn something about the electronic structure of functionalized tips. We showed that STM images obtained with a Xe-tip can be reproduced very well with s-like orbital on the PP [44] . On the other hand, we found that STM images acquired with CO-tips are well mimicked with p_x and p_y orbitals on the PP. Gross et al. [82] achieved good agreement for STM images obtained with CO tips in the far distance regime by taking into account linear combination of s, p_x and p_y orbitals on the probe. Pavlíček et al. [83] claimed that the p and s contributions can depend on the applied bias voltage.